

Dependence of the π -electron eigenvalue sum on the number of atoms in almost spherical C cages

C. Amovilli,¹ I. A. Howard,² D. J. Klein,³ and N. H. March^{2,4}

¹*Dipartimento di Chimica e Chimica Industriale, Università di Pisa, Via Risorgimento 35, 56126 Pisa, Italy*

²*Department of Physics, University of Antwerp (RUCA), Groenenborgerlaan 171, B-2020 Antwerp, Belgium*

³*Department of Marine Sciences, Texas A&M University, Galveston, Texas 77553*

⁴*Oxford University, Oxford, England*

(Received 6 March 2002; published 30 July 2002)

A free-electron-like model is first shown to lead to the eigenvalue sum of the π electrons in almost spherical C cages, being proportional to N , where N is the number of C atoms. The model is also closely related to a tight-binding model, stemming from the Hückel theory of π electrons. The equilibrium radius R_e of the C cages is assumed to be determined by the “rule” of constant surface area per C atom, and hence $R_e \propto N^{1/2}$. We then compare these models with a series of Hartree-Fock calculations on the fullerenes C_{50} , C_{60} , C_{70} , and C_{84} , from which more accurate energy scaling relations are obtained. Finally, the relation between the total energy of the four C cages at equilibrium and the all-electron eigenvalue sum is confirmed by the Hartree-Fock studies.

DOI: 10.1103/PhysRevA.66.013210

PACS number(s): 36.40.Cg, 73.61.Wp, 71.20.Tx, 61.48.+c

I. BACKGROUND AND OUTLINE

We have been independently examining quite different models for treating the π electrons in buckminsterfullerene and related almost spherical C cages [1,2]. In the first of these references, the so-called March model of fullerene [3–5] was employed; however, it was employed in its simplest form, in which self-consistency was not imposed. Therefore, here we shall turn to the second model of a quite different kind, namely, that of free π electrons confined to the surface of a sphere [6–10].

The π levels, in zeroth order, are those of a rigid rotator, having degeneracy $(2j+1)$ and energies $\hbar^2 j(j+1)/2I$ with I the moment of inertia. With double occupancy up through the n th shell, one then finds a total energy proportional to

$$2 \sum_{j=0}^n j(j+1)(2j+1) = n(n+1)^2(n+2), \quad (1)$$

which is easily confirmed in the limit of large N by replacing the summations by integration. With the identification of I as mR^2 ,

$$E_\pi = \frac{n(n+1)^2(n+2)\hbar^2}{2mR^2}. \quad (2)$$

Below, we shall insert an (approximate) equilibrium cage radius [see Eqs. (4) and (5) below] and, recognizing the total number of electrons as $2 \sum_{j=0}^n (2j+1) = 2(n+1)^2$, we find

$$E_\pi = \frac{\hbar^2 N}{8mk_e^2} - \frac{\hbar^2}{4mk_e^2}, \quad (3)$$

which is plainly the correct general form for a graphene sheet. A similar lead N dependence is also obtained for the simple Hückel tight-binding model [11], wherein there is a resonance integral β between each site and its three nearest neighbors. Indeed, by the Gerschgorin circle theorem, all the MO eigenvalues must be bound between $-3|\beta|$ and $+3|\beta|$ so

that the total N electron ground-state energy must be bounded between $-3|\beta|N$ and $+3|\beta|N$. Moreover, the MO levels are anticipated to be not too nonuniformly distributed so that the ground state is $\cong -CN$ (with $C \neq 0$ and probably not too different from $3|\beta|/2$, as indicated in Ref. [12]). To reach Eq. (3), we have used an “equilibrium” radius R_e determined by the “rule” that the surface area per C atom remains constant as the cage size becomes larger through an increase in the number of C atoms N . This means that

$$\frac{4\pi R_e^2}{N} = \text{const} \quad (4)$$

or

$$R_e = k_e N^{1/2}, \quad (5)$$

where k_e is a constant, which can evidently be fitted to the experimental value of R_e for buckminsterfullerene itself with $N=60$ (see also Table I below). Substituting Eq. (5) into Eq. (2) then yields Eq. (3) above.

An alternative argument can be given from two-dimensional Thomas-Fermi theory. Suppose the π electrons are modeled as a uniform distribution spread over the almost spherical cage. Then the kinetic energy T is given by [13]

TABLE I. Ground-state energy E and sum of eigenvalues for π electrons E_π in atomic units, and equilibrium radii R_e in Å for the four cages for which Hartree-Fock data has been obtained. N is the number of C atoms in the cage.

N	50	60	70	84
E/N	-37.5884	-37.6029	-37.5926	-37.5874
E_π/N	-0.2232	-0.2275	-0.2234	-0.2223
R_e	3.278	3.582	3.865	4.256
R_e/\sqrt{N}	0.463	0.462	0.462	0.464

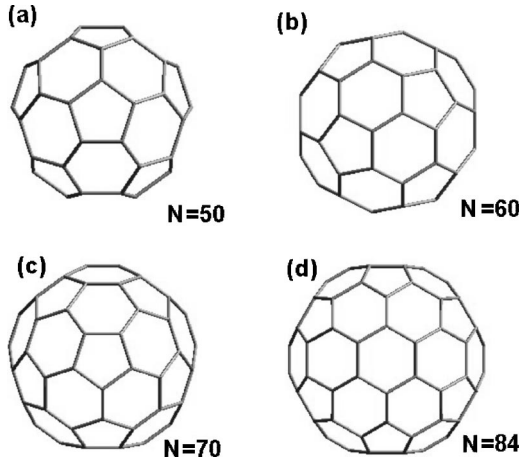


FIG. 1. Structure of the buckminsterfullerene (b), and also the (assumed) high symmetry structures of C_{50} (a), C_{70} (c), and C_{84} (d) used here.

$$T = A c_k^{(2)} n^2, \quad c_k^{(2)} = \frac{\pi \hbar^2}{2m}, \quad (6)$$

where A is the area and n is the number of π electrons per unit area, i.e.,

$$n = \frac{N}{4\pi R^2}. \quad (7)$$

Thus, the total kinetic energy is given by

$$T = (4\pi R^2) \frac{c_k^{(2)} N^2}{(4\pi R^2)^2} = \frac{c_k^{(2)} N^2}{4\pi R^2} = \frac{\hbar^2 N^2}{8mR^2}, \quad (8)$$

and by again using Eq. (5), we find $T \propto N$. Since in the “rigid-rotator-like” model all the energy is kinetic, we confirm Eq. (3) to leading order by the simplest form of density functional theory.

This is the point at which we shall bring these simple model predictions into contact with quantitative Hartree-Fock (HF) calculations on four C cages, namely, C_{50} , C_{60} , C_{70} , and C_{84} . This is done in Sec. II below. Section III presents a relationship between total energy E and eigenvalue sum E_s . Section IV constitutes a summary with some suggestions for possible future work.

II. HARTREE-FOCK STRUCTURES OF SOME C CAGES

A. Structures taken for four C cages and computational details

For C_{60} it is, of course, well established that the lowest isomer is the European football configuration. For C_{84} , we have used the work of Manolopoulos and Fowler [14], in which a whole variety of isomers were classified. The one we have chosen (albeit with some inevitable arbitrariness) is that of the highest symmetry. The nuclear framework is depicted in Fig. 1(d). For C_{70} , similar symmetry considerations led us to study the nuclear structure in Fig. 1(c), while the framework adopted for C_{50} is depicted in Fig. 1(a) (see also Schmalz *et al.* [15]).

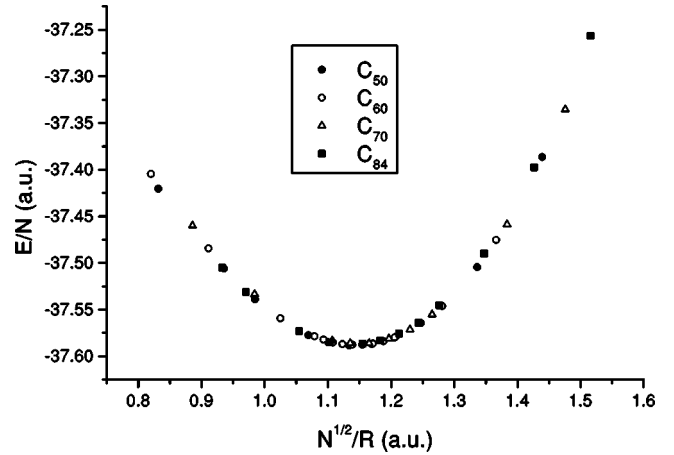


FIG. 2. Total HF energy E/N plotted vs $N^{1/2}/R$ for all four cages. The curves for the individual cages have been shifted by a constant to bring them into coincidence.

As a first step toward understanding overall structural effects of fullerene cages, we report Hartree-Fock energetics of these four C cages constrained to a spherical shape—i.e., with all the nuclei at a common distance R from the center. The Hartree-Fock energies have been obtained using the MINI-I basis set. We discuss our findings below. While our Hartree-Fock calculations involve all electrons, they will yield further insight into this field of C clusters to also extract information directly concerned with the π electrons.

B. Scaling of total energy curves for the four C cages

It turns out that the Hartree-Fock total energy $E(N, R)$, where N denotes the number of C atoms and R denotes the cage radius, can be well represented by the form

$$\frac{E(N, R)}{N} = a + b \frac{N^{1/2}}{R} + c \frac{N}{R^2}, \quad (9)$$

as shown in Fig. 2 for the four cages. In this figure, the four curves have been shifted by a small constant to bring them into coincidence. At the equilibrium radii, precise numerical values of E/N for the four cages are collected in Table I. Naturally, there is chemistry in the small differences between the total energy per carbon atom E/N versus N in the higher decimal places of the HF results. The “law” of constant surface area per C atom for the equilibrium radius embodied in Eq. (4) is already clear from Fig. 2 and is confirmed in the final row of Table I. The sum of occupied orbital energies E_s is plotted in Fig. 3, where it is shown that there is remarkable scaling of the four cages; the solid curve corresponds to the same Eq. (9) with parameters recorded in Fig. 3.

C. π -electron energies

Next, we have extracted the π -eigenvalue sum for the C cages. The reader will note that, owing to the curvature, in spherical clusters it is not possible to immediately identify the π orbitals among the canonical HF orbitals. Our π -eigenvalue sum, for a given C_n cage, corresponds to the

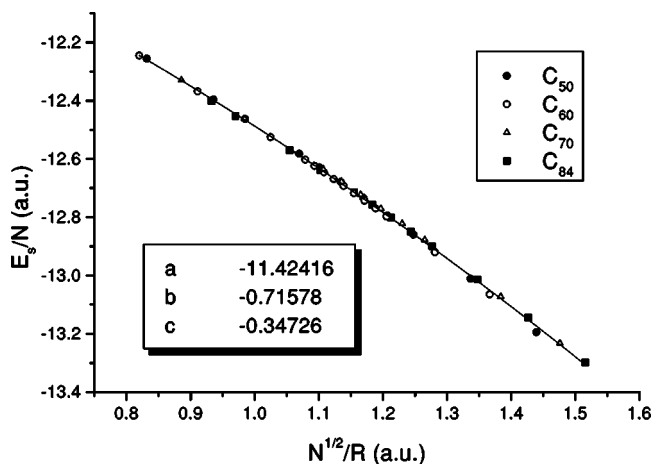


FIG. 3. Eigenvalue sums E_s/N plotted vs $N^{1/2}/R$ for C_{50} , C_{60} , C_{70} , and C_{84} . Values for the parameters a , b , and c representing the best fit to Eq. (9) for the composite curve are recorded. The curves have been shifted by a constant as in Fig. 2.

sum over the n canonical orbitals, which show the highest projection over a set of n p -like atomic functions orthogonal to the spherical cage surface. The four values of E_π/N at equilibrium are also recorded in Table I and show remarkable constancy. Presumably, the constant number already reflects the value anticipated to hold for a single graphene sheet, although, of course, the largest value of N in Table I is only 84. Figure 4 shows the π -electron eigenvalue sum for the four cages.

III. RELATION BETWEEN TOTAL ENERGY AND EIGENVALUE SUM OF ALL ELECTRONS: HF RESULTS AT THE EQUILIBRIUM CAGE RADII

To conclude this discussion of the HF results, we have examined the relation between total energy $E(N, R_e)$ and eigenvalue sum $E_s(N, R_e)$ (now of all electrons) for the four C cages on which we have HF data. The motivation for this goes back to March and Plaskett's [16] study on atoms. They

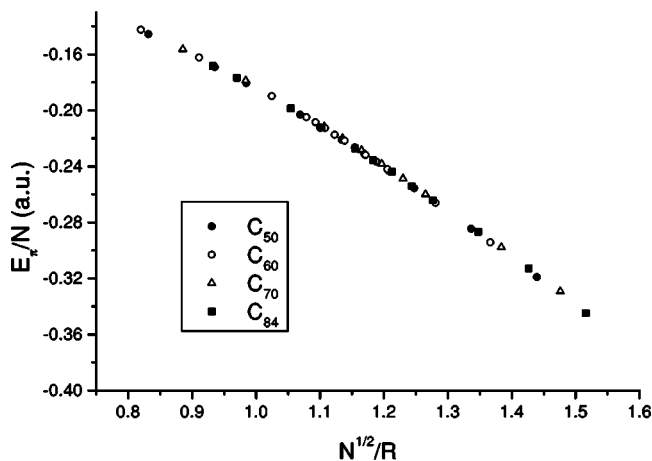


FIG. 4. π -electron eigenvalue sums E_π/N vs $N^{1/2}/R$ for C_{50} , C_{60} , C_{70} , and C_{84} . The curves have been shifted by a constant as in Fig. 2.

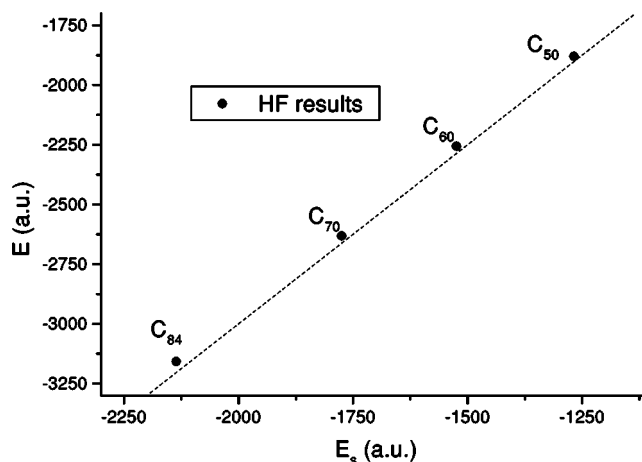


FIG. 5. Total HF energy E vs eigenvalue sum E_s at the equilibrium radius R_e for C_{50} , C_{60} , C_{70} , and C_{84} . The dashed line represents $E = (3/2)E_s$.

showed, using the simplest form of density functional theory, namely, the Thomas-Fermi statistical method, that

$$E = \frac{3}{2}E_s. \quad (10)$$

This relation was later shown by Ruedenberg [17] (see also March [18]) to be well obeyed by self-consistent calculations on a variety of molecules at their equilibrium geometry. Therefore, in Fig. 5 we have plotted $E(N, R_e)$ versus the all-electron eigenvalue sum $E_s(N, R_e)$. There is indeed a linear relation, and the dashed line is drawn with slope 3/2 for comparison. The fit is seen to be quantitative.

IV. SUMMARY AND POSSIBLE DIRECTIONS FOR FURTHER STUDY

The main achievements of this study of spherical cages can be summarized as follows. First, the total energy, the eigenvalue sum, and the π -electron eigenvalue sum as a function of N and R can be fitted accurately by the form (9). As seen from Fig. 3, for the total eigenvalue sum E_s there is quite remarkably accurate scaling relating all four cages. We believe this scaling should be robust against later changes in isomer structures for C_{50} , C_{70} , and C_{84} when the lowest energy structure is experimentally established. Second, we have extracted the π -electron eigenvalue sum at the equilibrium cage radii (see Table I). These, in the form of E_π/N , are already remarkably constant and, even though N is small, we expect constancy to have already been closely approached. Third, the relation (10) between the total energy and the eigenvalue sum, for all electrons, calculated at the equilibrium radii, is demonstrated to hold almost quantitatively for the four cages studied.

Typically, there will be notable anisotropic curvature for fullerenes at equilibrium geometry. To see this, first consider a best candidate for uniform curvature: this is a fullerene with the pentagonal "defects" spread as uniformly as possible, that is, an icosahedral-symmetry fullerene. For such a fullerene (which we imagine for the large- N limit), the pentagons may be viewed to be at the corners of an icosahedron-

like superstructure, with all other rings being hexagons. Then consider a graphitic region corresponding to one of the triangular faces of the icosahedronlike superstructure. The area of this face (there being 20 such faces), as measured on the surface of a (uniformly curved) spherical surface of radius R , is

$$A_{\text{curved}} = \frac{4\pi R^2}{20}. \quad (11)$$

The length of the side of such a spherical triangle is $l = \theta R$, where θ is the angle subtended by the edge as viewed from the center of the sphere. The area of a planar triangle with the same length edges is $A_{\text{flat}} = (l/2)(\sqrt{3}/4l)$. But A_{flat} (as would correspond to an unstrained section of the graphitic lattice) and A_{curved} do not agree; there is a strain per carbon atom of

$$\sigma \sim \sqrt{A_{\text{flat}}/(N/20)} - \sqrt{A_{\text{curved}}/(N/20)}. \quad (12)$$

This strain occurs for each bond in the graphitic portion of the network. So with about $3N/2$ such bonds, the total stress is $E_{\text{stress}} \approx (3N/2)1/2k\sigma^2$ with k as some suitable force constant (for C—C aromatic bonds). Thus,

$$E_{\text{stress}} \sim 15k \left(\frac{3^{1/4}}{2} \theta - \sqrt{\frac{\pi}{5}} \right)^2 R^2. \quad (13)$$

But $R^2 \propto N$, so that stress is quite important, and can even give a correction beyond that of bulk graphite if unrelieved, as with the spherically curved surface. If a structure other than that of icosahedral symmetry for the arrangement of the pentagons is presumed, then the geometric factor above is modified, but still nonzero.

The question of relief of curvature strain then arises (still in the limit of large N). Again as a representative example, the icosahedral symmetry arrangement may be considered. One simply imagines that the structure deforms to look like an icosahedron superstructure with the pentagons at the apices. That is, the triangular graphitic regions of the preceding paragraph are imagined to be changed from the spherically curved form of the preceding paragraph to near planar regions with anisotropic curvature at the edges connecting each triangular region to adjacent ones. Then, within the pla-

nar triangular regions there is no strain and no stress; instead, it all occurs at the edges of the triangles. Clearly, the total amount of such edge is $\approx 30R \sim N^{1/2}$ so that now we have a structure with less stress, $E'_{\text{stress}} \sim N^{1/2}$. Again, the proportionality depends on the particular manner of dispersal of the pentagons, the overall conclusion being that geometric Gaussian curvature is [2] preferably localized in the region of the pentagons with then anisotropic curvature (without Gaussian curvature) mediating between such neighboring regions. Notably for computations [19] on large non-open-shell icosahedral-symmetry fullerenes, the suggested polyhedralization can be clearly perceived in diagrams of the geometry optimized structures (most clearly for the largest treated, at $N = 540$).

We have already referred to the urgent need to settle the question of the lowest isomer structures for C_{50} , C_{70} , and C_{84} . This presently appears to be a task for experimentation (see [20]). Current theoretical approaches lack the power to decisively distinguish between isomer structures that will differ very little in energy. A final comment concerns connectivity theory. Beyond the constancy of the values of E_{π}/N in Table I, we conclude that a correction term of $\mathcal{O}(1/\sqrt{N})$ could exist. However, using the HF values, the behavior is not monotonic. For several approximations within the connectivity (or Hückel) theory, a term of $\mathcal{O}(1/\sqrt{N})$ is present in the study by Gutman and Soldatović [21], though their approximations are gauged against a set of (~ 100) benzenoids (without pentagonal rings).

ACKNOWLEDGMENTS

C.A. wishes to acknowledge the hospitality at the RUCA campus of the University of Antwerp during the period in which this investigation was completed. I.A.H. wishes to acknowledge support from the Flemish Science Foundation (FWO) under Grant No. G.0347.97. We also thank the University of Antwerp (RUCA) for its support in the framework of the Visiting Professors Program. This work is also supported by the Concerted Action Program of the University of Antwerp. N.H.M. acknowledges financial support from the Francqui Foundation. Thanks are especially due to the Executive Director, Professor L. Eyckmans, for his help and encouragement. D.J.K. acknowledges the support of the Welch Foundation of Houston, Texas.

-
- [1] I. A. Howard and N. H. March, in *Reviews in Modern Quantum Chemistry: A Celebration of the Contributions of R. G. Parr*, edited by K. D. Sen (World Scientific, Singapore, in press).
- [2] D. J. Klein and H.-Y. Zhu, in *From Chemical Topology to Three-Dimensional Topology*, edited by A. T. Balaban (Plenum, New York, 1997), pp. 297–341.
- [3] D. P. Clougherty and X. Zhu, *Phys. Rev. A* **56**, 632 (1997).
- [4] F. Despa, *Phys. Rev. B* **57**, 7335 (1998).
- [5] F. Siringo, G. Piccitto, and R. Pucci, *Phys. Rev. A* **46**, 4048 (1992).
- [6] R. C. Haddon, L. E. Brus, and K. Raghavachari, *Chem. Phys. Lett.* **125**, 459 (1985).
- [7] M. Ozaki and A. Takahashi, *Chem. Phys. Lett.* **127**, 242 (1986).
- [8] E. Brensdal, S. J. Cyrin, B. N. Cyrin, J. Brunvoll, D. J. Klein, and W. A. Seitz, in *Quasicrystals, Networks, and Molecules of Five-Fold Symmetry*, edited by I. Hargittai (VCH, New York, 1990), pp. 257–276.
- [9] R. Saito, G. Dresselhaus, and M. S. Dresselhaus, *Phys. Rev. B* **46**, 9906 (1992).
- [10] M. R. Savina, L. L. Lohr, and A. H. Francis, *Chem. Phys. Lett.* **205**, 200 (1993).
- [11] See, for instance, C. A. Coulson, R. B. Mallion, and B.

- O'Leary, *Hückel Theory for Organic Chemists* (Academic, London, 1978).
- [12] I. Gutman, A. Nikolić, and Z. Tomović, *Chem. Phys. Lett.* **349**, 95 (2001).
- [13] N. H. March, *Electron Density Theory for Atoms and Molecules* (Academic, New York, 1992), p. 173.
- [14] D. E. Manolopoulos and P. W. Fowler, *J. Chem. Phys.* **96**, 7603 (1992).
- [15] T. G. Schmalz, W. A. Seitz, D. J. Klein, and G. E. Hite, *J. Am. Chem. Soc.* **110**, 1113 (1988).
- [16] N. H. March and J. S. Plaskett, *Proc. R. Soc. London, Ser. A* **235**, 419 (1956).
- [17] K. Ruedenberg, *J. Chem. Phys.* **66**, 375 (1977).
- [18] See also N. H. March, *J. Chem. Phys.* **67**, 4618 (1977).
- [19] D. Bakowies and W. Thiel, *J. Am. Chem. Soc.* **113**, 3704 (1991).
- [20] S. J. LaPlaca, P. A. Roland, and J. J. Wynne, *Chem. Phys. Lett.* **190**, 163 (1992).
- [21] I. Gutman and T. Soldatović, *Commun. Math. Chem.* **44**, 169 (2001).